Global escalation of more frequent and intense compound heatwave-extreme precipitation events

Haoyu Jin [1,2,3,9*], Ke Zhang [1,3,4,5,6*], Moyang Liu [7], Xuan Yu [8], Xu Yang [1,4], Lijun Chao [1,4], Pengfei Zhang [1,4], Guoyan Liu [1,4]

[1] State Key Laboratory of Water Disaster Prevention, Hohai University, Nanjing, Jiangsu, 210024, China

[2] Key Laboratory of Transportation Meteorology of China Meteorological Administration, Nanjing Joint Institute for Atmospheric Sciences, Nanjing 210041, China

[3] Yangtze Institute for Conservation and Development, Nanjing, Jiangsu, 210024, China

[4] College of Hydrology and Water Resources, Hohai University, Nanjing, Jiangsu, 210024, China

[5] China Meteorological Administration Hydro-Meteorology Key Laboratory, Hohai University, Nanjing, Jiangsu, 210024, China

[6] Key Laboratory of Water Big Data Technology of Ministry of Water Resources, Hohai University, Nanjing, Jiangsu, 210024, China

[7] The Fenner School of Environment and Society, The Australian National University (ANU), Canberra, ACT 0200, Australia

[8] State Key Laboratory of Soil and Sustainable Agriculture, Institute of Soil Science, Chinese Academy of Sciences, Nanjing 210008, China

[9] Meteorological Administration Hydro-Meteorology Key Laboratory, China

*** Correspondence:** Haoyu Jin (haoyu.jin@hhu.edu.cn) and Ke Zhang (kzhang@hhu.edu.cn)

Abstract. Compound heatwave-extreme precipitation (CHWEP) events, the rapid succession of heatwaves and extreme precipitation, pose growing compound and cascading risks. However, global-scale comparisons of their spatiotemporal evolution against single extremes remain limited. This study systematically examines the changes in CHWEP and corresponding single extremes from 1980 to 2100 using climate observations and projections under SSP (Shared Socioeconomic

Pathway) 2-4.5 and SSP5-8.5 scenarios. We find that CHWEP exhibit higher frequency, stronger precipitation, and longer heatwave duration in mid-to-high latitudes of the Northern Hemisphere, while tropical CHWEP feature more intense heatwaves than single heatwave events. These spatial contrasts persist in future projections. Under both scenarios, CHWEP and single extreme metrics intensify globally by 2056-2100, with post-heatwave precipitation exceeding that of single precipitation extremes, particularly under SSP5-8.5, highlighting sensitivity to greenhouse forcing. Critically, the co-occurrence is non-random, indicating an emerging physical linkage. In the tropics, the likelihood of extreme rainfall following heatwaves increases markedly. Our findings demonstrate that CHWEPs are evolving into a distinct, intensifying hazard class, necessitating their integration into climate resilience, early warning, and adaptation frameworks.

1 Introduction

Global warming has significantly increased the frequency and intensity of extreme climate events, posing growing threats to human societies and ecosystems (Diffenbaugh et al., 2017; Gu et al., 2022; Myhre et al., 2019). Among these, heatwaves and extreme precipitation are two of the most widespread and hazardous types of extreme weather (Raghavendra et al., 2018; Sun et al., 2024). They are typically treated as independent phenomena, as their physical mechanisms and manifestations are contrasting, and they rarely occur simultaneously at the same location (Sauter et al., 2023a; Sun et al., 2023). However, a non-synchronous but causally linked lagged response may exist between them. For instance, prolonged heatwaves can alter land-atmosphere interactions, such as inducing soil drying, enhancing boundary layer warming, and accumulating convective instability energy, thereby creating favorable conditions for subsequent extreme precipitation, forming a "heat-then-rain" compound event chain (Chen et al., 2022; Li et al., 2025; Liu et al., 2024; Yang and Yuan, 2025).

The concept of compound extreme events was first introduced in the IPCC (Intergovernmental Panel on Climate Change) Fifth Assessment Report (AR) and has been further refined in AR6 into four categories: multivariate, multi-event, temporally compounding, and spatially compounding extremes (Bevacqua et al., 2023; Fang et al., 2025; Fischer and Knutti, 2015). Studies have shown that the impacts of compound events often far exceed the simple sum of individual extremes, exhibiting significant nonlinear amplification effects (Ning et al., 2022; Zhao et al., 2022). Among these, compound heatwave-extreme precipitation (CHWEP) events have attracted increasing attention due to their potential to trigger "drought-to-flood" transition disaster chains (Ganguli and Merz, 2024; Götte and Brunner, 2024; Sauter et al., 2023b; Zhou et al., 2023). In this study, we primarily focus on heatwaves and extreme precipitation events that are temporally consecutive, i.e., CHWEP events defined by their temporal linkage. However, current research is largely limited to regional case studies, and the global spatiotemporal patterns, trends, and underlying drivers of CHWEP events remain poorly understood, especially in comparison with single extreme events (Jin et al., 2024; Mazdiyasni and AghaKouchak, 2015; Miao et al., 2024). More critically, the future changes in the occurrence probability, intensity, and associated compound risks of CHWEP events under a warming climate remain largely unexplored and constitute a major knowledge gap (Séférian et al., 2019; Xiong et al., 2023; You and Wang, 2021; Zscheischler et al., 2018).

In this study, based on multiple reanalysis datasets and the multi-model ensemble from the Coupled Model Intercomparison Project Phase 6 (CMIP6), we define CHWEP events along with their corresponding single heatwave and extreme precipitation events. First, we systematically compare the historical changes (1980-2024) and future projections (2056-2100) in the frequency, intensity, and duration of CHWEP events and their single-component counterparts at the global scale. Second, we investigate the potential linkage between heatwaves and extreme precipitation events through probabilistic analysis, demonstrating that CHWEP events are not merely the result of random co-occurrence. This study systematically analyzes the spatiotemporal differences in the changes of CHWEP and individual extreme events between historical and future periods, with a particular focus on the distinctions between CHWEP events and single extreme events. This research can provide critical scientific support for extreme weather early warning systems and holds significant practical implications for enhancing societal climate resilience.

In the remainder of this manuscript, Section 2 describes the three reanalysis datasets and four CMIP6 global climate models (GCMs) used to identify temporally consecutive CHWEP events. Section 3 presents the methodologies for defining single heatwave, single extreme precipitation, and CHWEP events, determined by temperature thresholds, extreme precipitation thresholds, and a time window. And further examines the statistical significance of differences among metrics of different event types, as well as the randomness of their co-occurrence. Section 4 presents the results along with interpretability analyses. Section 5 discusses key insights derived from this study. Finally, Section 6 provides the concluding remarks.

2 Data

In this study, we selected three global reanalysis datasets: ERA5-Land (Sun et al., 2024), MERRA-2 (Chen et al., 2019), and JRA-55 (KOBAYASHI et al., 2015), which are widely used in climate research, weather forecasting, hydrological modeling, and extreme event analysis (Chen et al., 2019; Huang et al., 2015; Wang et al., 2019a). These three reanalysis datasets provide daily-scale precipitation data as well as daily-scale maximum temperature data, meeting the requirements of this study. Daily precipitation and daily maximum temperature data from 1980 to 2024 were used. Due to differences in spatial resolution and performance among the datasets, we resampled all data to a uniform 1° × 1° grid using kriging interpolation and the average of three reanalysis datasets is used as the final input to identify single extreme events and CHWEPs. To analyze the future evolution of CHWEP events, we used daily precipitation and daily maximum temperature outputs from four CMIP6 GCMs for the period 2056-2100, under two Shared Socioeconomic Pathway (SSP) scenarios: SSP2-4.5 (representing a medium emission scenario) and SSP5-8.5 (representing a high emission scenario) (Table S1) (Balaji et al., 2018; Juckes et al., 2020). These four GCMs offer relatively high accuracy and spatial resolution, and more importantly, they provide daily maximum temperature datasets under the future SSP2-4.5 and SSP5-8.5 scenarios. Similarly, the model data were interpolated to a 1° × 1° grid using kriging, and the multi-model mean was computed to identify single extreme events and CHWEPs (Hausfather et al., 2022).

3 Methods

3.1 Precipitation and temperature deviation correction

Quantile delta mapping (QDM) is a statistical technique used for bias correction in climate modeling, particularly relevant for evaluating extreme weather events under changing climate conditions. It merges traditional quantile mapping (QM) principles with a delta change approach, ensuring that relative differences between quantiles from observational data and climate model outputs are preserved while addressing systematic biases inherent in climate projections. The QDM methodology encompasses two primary steps. It first applies a quantile mapping technique to adjust the bias of climate model outputs based on observed data. In this study, we use the historical-period (1980-2024) average of three reanalysis datasets as the reference baseline. Unlike traditional QM method, QDM preserves projected changes in the distribution of these quantiles across various conditions rather than simply replacing simulated values with observed ones based on corresponding quantiles. This results in outputs that better represent both historical and future states of climate data while maintaining the behavior of extreme weather phenomena, thus avoiding distortions that may occur with standard quantile mapping approaches. The bias correction formulas for precipitation and temperature are as follows:

$$p = F_{M,f}(x) \tag{1}$$

$$P_{QDM} = Q_R(p) \times \frac{Q_{M,f}(p)}{Q_{M,h}(p)} \tag{2}$$

$$T_{QDM} = Q_R(p) + [Q_{M,f}(p) - Q_{M,h}(p)] \tag{3}$$

where p is the cumulative probability, $F_{M,f}$ is the cumulative distribution function (CDF) of precipitation or temperature under the CMIP6 future scenario, and x is the precipitation or temperature value in the future period, P_{QDM} is the precipitation value after QDM bias correction, $Q_R(p)$ represents the quantile of precipitation or temperature in the reanalysis data corresponding to cumulative probability p, $Q_{M,f}(p)$ is the quantile of precipitation or temperature in the CMIP6 future simulation at cumulative probability p, and $Q_{M,h}(p)$ is the quantile of precipitation or temperature in the CMIP6 historical simulation at cumulative probability p, T_{QDM} is the temperature value after QDM bias correction. It is worth noting that since this study primarily focuses on the relative differences between CHWEP events and single extreme events, rather focus on absolute magnitudes, the precise accuracy of the absolute values does not affect the overall conclusions.

3.2 Identification and characteristics of CHWEP events

In this study, we first define heatwave events and extreme precipitation events. A heatwave is identified as a period of at least three consecutive days (≥3 days) during which the daily maximum temperature exceeds the 90th percentile threshold of historical daily maximum temperatures

(Wang et al., 2019b; Zscheischler et al., 2020). That is, the 90th percentile of the daily maximum temperature time series from 1980 to 2024 at each grid point is used as the threshold for defining heatwaves. Extreme precipitation is defined as a daily precipitation amount exceeding the 90th percentile threshold derived from all wet days (>1 mm) in the historical period. That is, the 90th percentile of the daily precipitation time series on wet days (>1 mm) from 1980 to 2024 at each grid point is used as the threshold for defining extreme precipitation events. The purpose of selecting the 90th percentile as the threshold is to obtain a sufficient number of heatwave and extreme precipitation event samples. In the future SSP2-4.5 and SSP5-8.5 scenarios, the thresholds for extreme precipitation and heatwave events are defined using the thresholds established during the historical period based on reanalysis data. The CHWEP event is characterized by the occurrence of an extreme precipitation event within 7 days following a heatwave event (You and Wang, 2021). This 7-day window is chosen to ensure a physically plausible linkage between the two events while maintaining a sufficient sample size for statistical analysis (Ridder et al., 2020; Sauter et al., 2023b). Events that do not meet the CHWEP criteria are classified as single heatwave or single extreme precipitation events (Fig. 1). We defined four metrics to quantify the characteristics of CHWEPs and individual extreme events (extreme precipitation and heatwaves) occurring within a given year: Frequency, Heatwave intensity, Extreme precipitation intensity, Duration. The calculation formulas are as follows:

$$F_C = \sum_{i=1}^{n_C} 1_i \tag{4}$$

$$F_S = \sum_{i=1}^{n_S} 1_i \tag{5}$$

$$IT_C = mean(\sum_{j}^{m_{CT}} T_{C-j}) \tag{6}$$

$$IT_s = mean(\sum_{j}^{m_{ST}} T_{S-j}) \tag{7}$$

$$IP_C = mean(\sum_{j}^{m_{CP}} P_{C-j}) \tag{8}$$

$$IP_S = mean(\sum_j^{m_{SP}} P_{S-j}) \tag{9}$$

$$D_C = mean(\sum_i^{n_C} D_{C-i}) \tag{10}$$

$$D_S = mean(\sum_i^{n_S} D_{S-i}) \tag{11}$$

where F denotes the annual frequency of CHWEPs or single heatwave events, IT represents the mean daily maximum temperature during the CHWEPs or single heatwave events in a year, IP denotes the mean precipitation amount during the CHWEPs or single extreme precipitation events in a year, and D refers to the duration of the heatwave in days during the CHWEPs or single heatwave events in a year, subscript C indicates CHWEP events, subscript S denotes single extreme events, n_C denotes the total number of occurrences of CHWEPs in a year, n_S denotes the total number of occurrences of single heatwave events in a year, m_{CT} denotes the total number of days with heatwaves within CHWEPs in a year, m_{ST} denotes the total number of days within heatwave events in a year, m_{CP} denotes the total number of days with extreme precipitation within CHWEPs in a year, m_{SP} denotes the total number of days within single extreme precipitation events in a year.

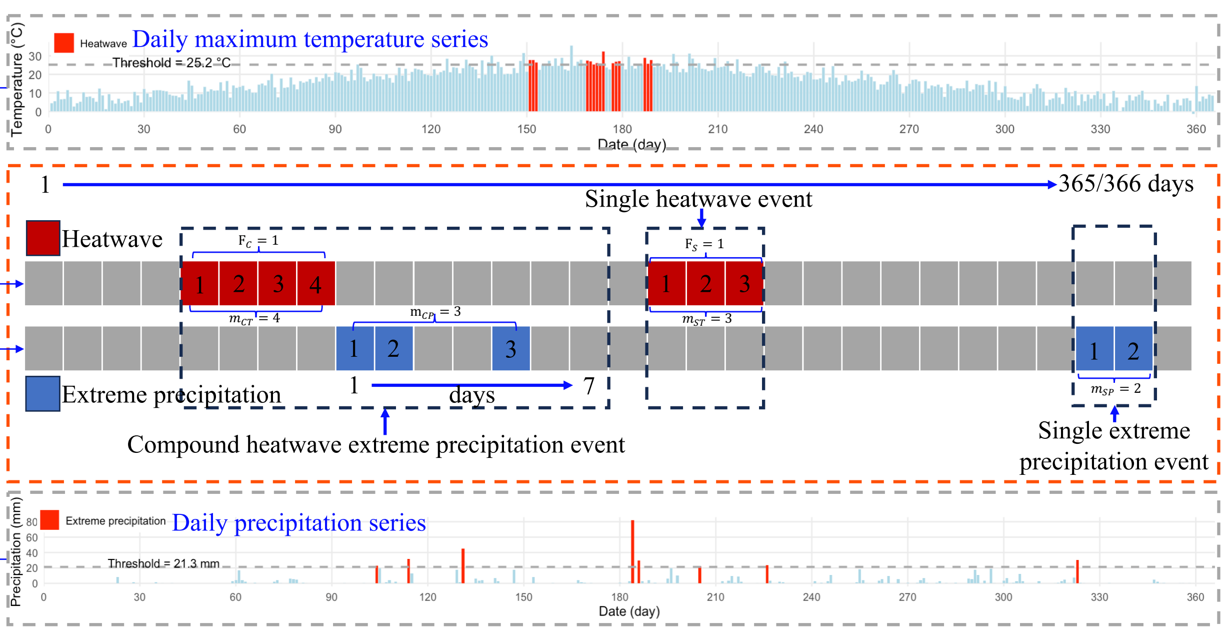

Figure 1. Schematic illustration of CHWEP and single extreme precipitation and heatwave events extracted from daily precipitation and daily maximum temperature time series over a year.

3.3 Significance test of median difference

In this study, the Wilcoxon rank-sum test (WRST) was employed to evaluate differences in the medians of extreme event characteristics. Comparisons were made between CHWEP and single extreme events, as well as between the future projection period (2056-2100) and the historical baseline (1980-2024). As a non-parametric method, the WRST assesses significant differences between two independent samples without assuming a specific data distribution (Guerreiro et al., 2018). This lack of distributional assumptions renders the test robust against skewed distributions, small sample sizes, and outliers. Consequently, the WRST is particularly suitable for analyzing extreme climate events, which often exhibit non-normal behavior and high variability (Babüroğlu et al., 2021; Dao, 2022).

3.4 Event coincidence analysis

CHWEP events may arise either from the random co-occurrence of heatwaves and extreme precipitation, or through a potential physical linkage whereby the occurrence of heatwaves promotes the subsequent development of extreme precipitation (Liu et al., 2024; Ning et al., 2022). To investigate the underlying mechanisms of CHWEP events, we employ event coincidence analysis (ECA). ECA is a statistical method designed to assess the potential associations between discrete events in two or more time series (Donges et al., 2016; Xiao et al., 2025). It is particularly effective in detecting whether events in different systems occur simultaneously or in close temporal proximity more often than expected by chance, thereby helping us determine whether there is a potential linkage between the events (Sun et al., 2024). The method quantifies the strength of such linkages by comparing the observed coincidence rate with the expected coincidence rate under randomness. The corresponding formulas are as follows:

$$P_{H\to P} = \frac{1}{N_H}\sum_{i=1}^{N_H} 1(\exists t_j^P \in P, 0 \le t_j^P - t_i^H \le \Delta) \tag{12}$$

$$P_{rand} = 1 - \exp(-\lambda_P \Delta) \approx \lambda_P \Delta = \frac{N_P \Delta}{T} \tag{13}$$

$$R = \frac{P_{H\to P}}{P_{rand}} \tag{14}$$

$$\sigma = \sqrt{\frac{1}{N}\sum_{i=1}^{N}(x_i - \bar{x})^2} \tag{15}$$

where $P_{H\to P}$ denotes the observed coincidence probability from heatwaves to extreme precipitation events, $H = \{t_i^H\}$ represents the set of occurrence times of heatwave events, N_H is the number of heatwave events occurring in a year, $P = \{t_j^P\}$ denotes the set of occurrence times of extreme precipitation events, with N_P being the number of such events in a year, Δ is the time window defining the allowable interval between a heatwave and a subsequent extreme precipitation event; in this study, it is set to within 7 days, P_{rand} represents the probability that extreme precipitation events occur randomly following heatwave events, λ_P is the average occurrence density of extreme precipitation events, defined as $\frac{N_P}{T}$, where T is the total observation period, in this study, the number of days in a year, i.e., 365 or 366. R is the ratio of $P_{H\to P}$ to P_{rand}. An R greater than 1 indicates that the observed probability is higher than the random probability. σ denotes the standard deviation (SD), N is the length of the sequence, x represents the variable, which in this study corresponds to $P_{H\to P}$, P_{rand}, and R, and $\bar{x}$ is the mean of the variable. We use the SD to quantify the interannual variability of $P_{H\to P}$, P_{rand}, and R, a larger SD indicates greater interannual variation in the variable (Adeloye et al., 2015).

4 Results

4.1 Historical comparison of CHWEP and single extreme events

CHWEPs exhibit distinct spatial frequency patterns compared to single heatwaves. CHWEPs occur more frequently in the mid- to high-latitude regions of the Northern Hemisphere (Fig. 2a), whereas single heatwaves are more prevalent in tropical regions, the western coastal region of the United States, Spain, northern Africa, the Middle East, and Central Asia (Fig. 2b). This may be because warming temperatures in the mid- to high-latitude regions of the Northern Hemisphere enhance the hydrological cycle, thereby promoting the occurrence of extreme precipitation events, whereas tropical or desert regions exhibit distinct wet and dry seasons, where individual heatwave events occur more frequently and last longer. The spatial patterns of heatwave intensity are broadly similar between CHWEPs (Fig. 2c) and single heatwaves (Fig. 2d), with hotspots in the Sahara Desert, the Middle East, and Australia. Similarly, the intensity patterns of extreme precipitation during CHWEPs (Fig. 2e) resemble those of single extreme precipitation events (Fig. 2f), with high-intensity regions located in the equatorial zone, northern Argentina, and southern China. The spatial distribution of heatwave duration also shows strong similarity between CHWEPs (Fig. 2g) and single heatwaves (Fig. 2h), with prolonged durations predominantly observed in the equatorial regions, the Middle East, and India. Additionally, we analyzed the changes in metrics across different regions based on continental boundaries (Fig. S1). Box plots of the frequency, heatwave intensity, extreme precipitation intensity, and heatwave duration for CHWEP and single extreme events in different regions are shown in Fig. S2.

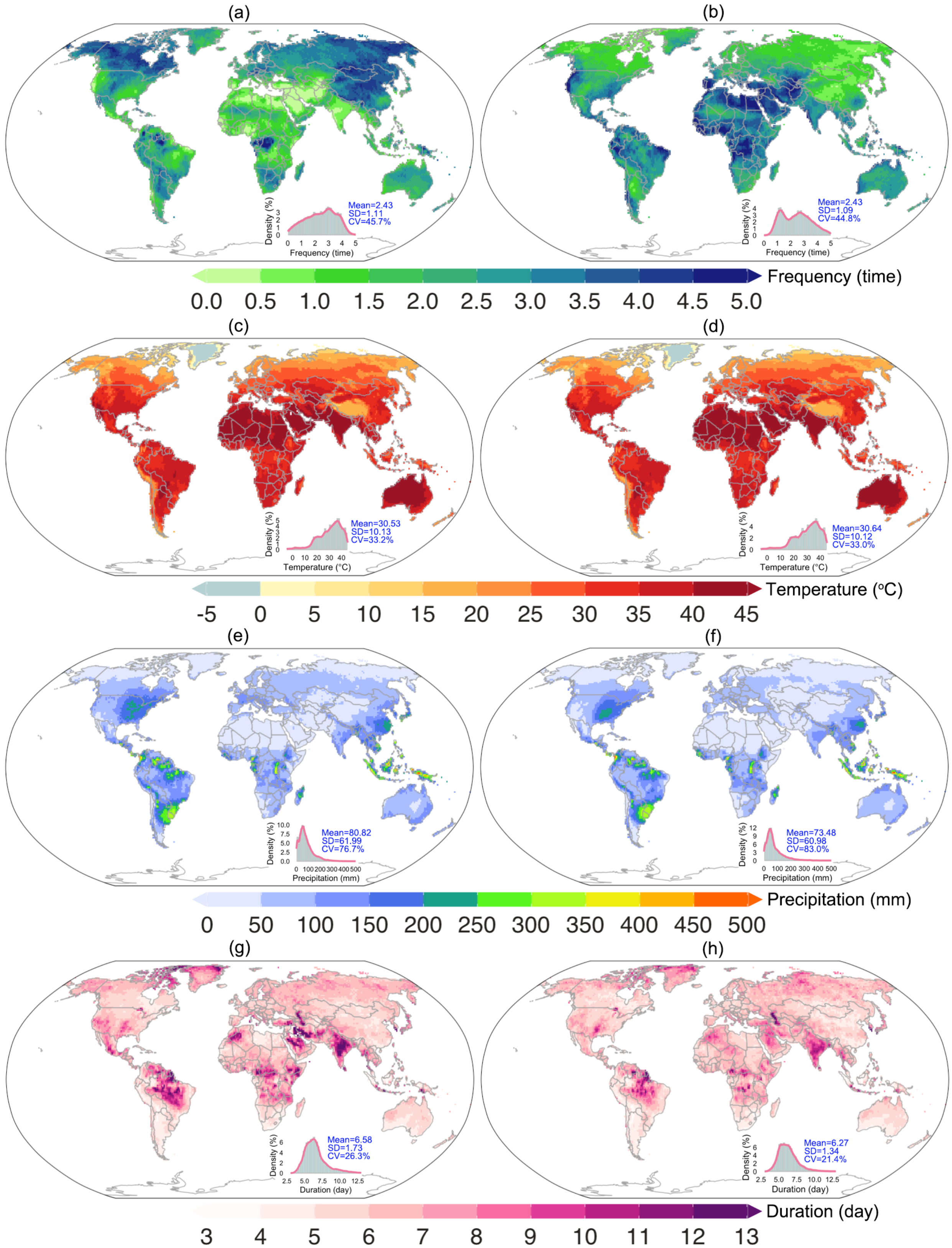

(a)
(b)
Mean=2.43
SD=1.11
CV=45.7%
Density (%)
Frequency (time)
Mean=2.43
SD=1.09
CV=44.8%
Density (%)
Frequency (time)
Frequency (time)
0.0 0.5 1.0 1.5 2.0 2.5 3.0 3.5 4.0 4.5 5.0
(c)
(d)
Mean=30.53
SD=10.13
CV=33.2%
Density (%)
Temperature (°C)
Mean=30.64
SD=10.12
CV=33.0%
Density (%)
Temperature (°C)
Temperature (°C)
-5 0 5 10 15 20 25 30 35 40 45
(e)
(f)
Mean=80.82
SD=61.99
CV=76.7%
Density (%)
Precipitation (mm)
Mean=73.48
SD=60.98
CV=83.0%
Density (%)
Precipitation (mm)
Precipitation (mm)
0 50 100 150 200 250 300 350 400 450 500
(g)
(h)
Mean=6.58
SD=1.73
CV=26.3%
Density (%)
Duration (day)
Mean=6.27
SD=1.34
CV=21.4%
Density (%)
Duration (day)
Duration (day)
3 4 5 6 7 8 9 10 11 12 13

Figure 2. Spatial distribution of the mean values of the frequency (a and b), heatwave intensity (c and d), extreme precipitation intensity (e and f), and heatwave duration (e and f) of CHWEP (a, c, e, and g) and single extreme events (b, d, f, and h) from 1980 to 2024.

CHWEPs occur more frequently than single heatwaves in mid-to-high latitude regions (Fig. 3a). The heatwave intensity associated with CHWEPs is significantly higher than that of single heatwaves in tropical regions (Fig. 3b). In most mid- to high-latitude regions of the Northern Hemisphere, the extreme precipitation intensity during CHWEPs exceeds that of single extreme precipitation events (Fig. 3c). Moreover, the duration of heatwaves within CHWEPs is notably longer than that of single heatwaves in the mid-to-high latitudes (Fig. 3d). These results indicate that the impacts of CHWEPs are more pronounced in mid-to-high latitude regions compared to low latitudes. Box plots of the median differences between CHWEP and single extreme events in frequency, heatwave intensity, extreme precipitation intensity, and heatwave duration across different regions from 1980 to 2024 are shown in Fig. S3.

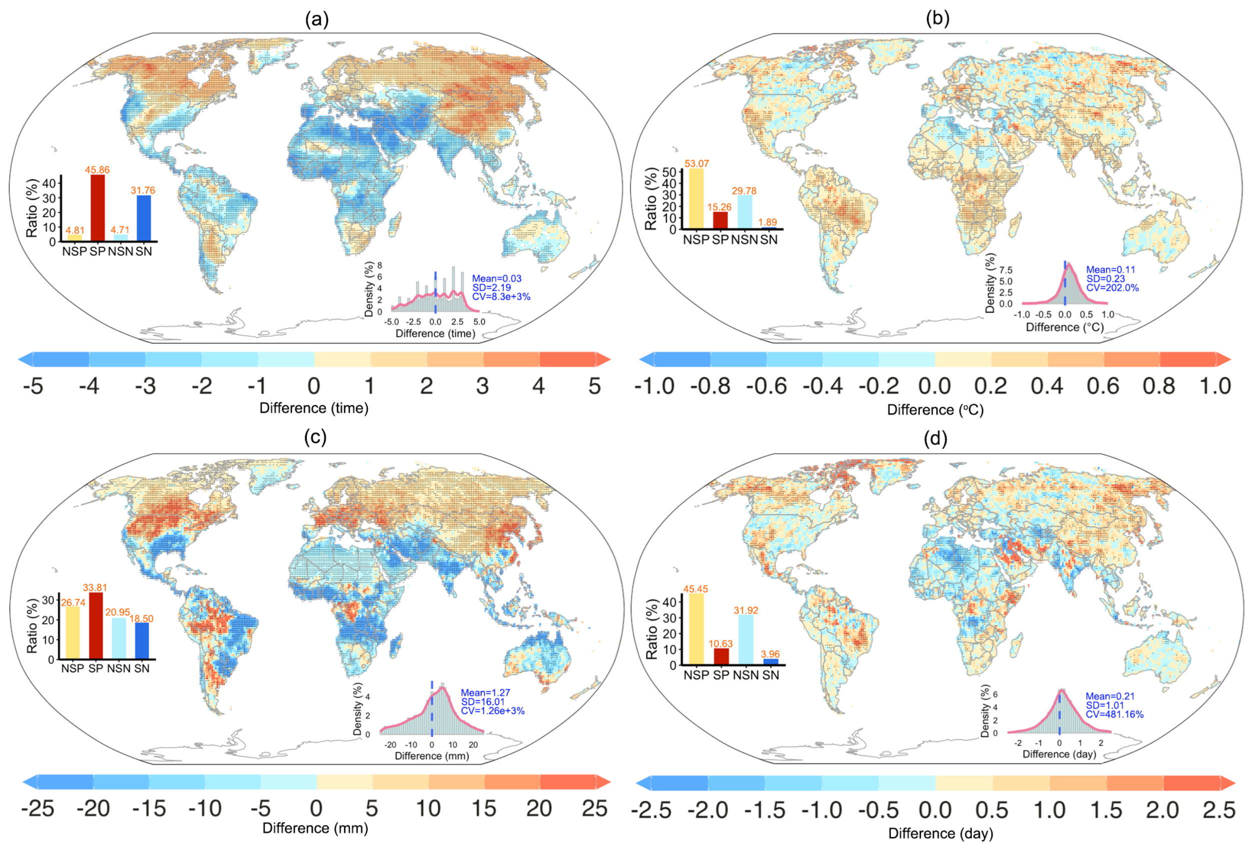

Figure 3. Spatial distribution of median differences between CHWEP and single extreme events in frequency (a), heatwave intensity (b), extreme precipitation intensity (c), and heatwave duration (d) from 1980 to 2024. (Note: In the left bar chart, NSP denotes Non-Significant Positive, SP denotes Significant Positive, NSN denotes Non-Significant Negative, and SN denotes Significant Negative. The same abbreviations apply hereinafter.)

4.2 Future changes and comparisons of CHWEP and single extreme events

Under the SSP2-4.5 (Fig. S4) and SSP5-8.5 (Fig. S5) scenarios, the spatial patterns of CHWEPs and single extreme events are broadly similar to those observed during the historical period (Fig. 2), indicating a consistent spatial organization of extreme events across time periods. South America (SAM) exhibits the strongest precipitation intensity in both CHWEP and single extreme precipitation events, but the shortest heatwave duration (Fig. S6). The spatial distribution of differences in event characteristics between CHWEPs and single extremes also remains largely unchanged under future projections. Specifically, the frequency of CHWEPs (Fig. 4a), the intensity of associated extreme precipitation (Fig. 4e), and heatwave duration (Fig. 4g) are substantially higher in mid-to-high latitudes compared to single events (Fig. 4b, f, and h). Conversely, heatwave intensity during CHWEPs is greater in tropical regions than that of single heatwaves (Fig. 4c and d). Notably, the magnitude of these differences is more pronounced under the SSP5-8.5 scenario than under SSP2-4.5, suggesting an amplification of compound event characteristics under stronger warming. The median differences in metrics between CHWEP and single extreme events across different regions are shown in Fig. S7.

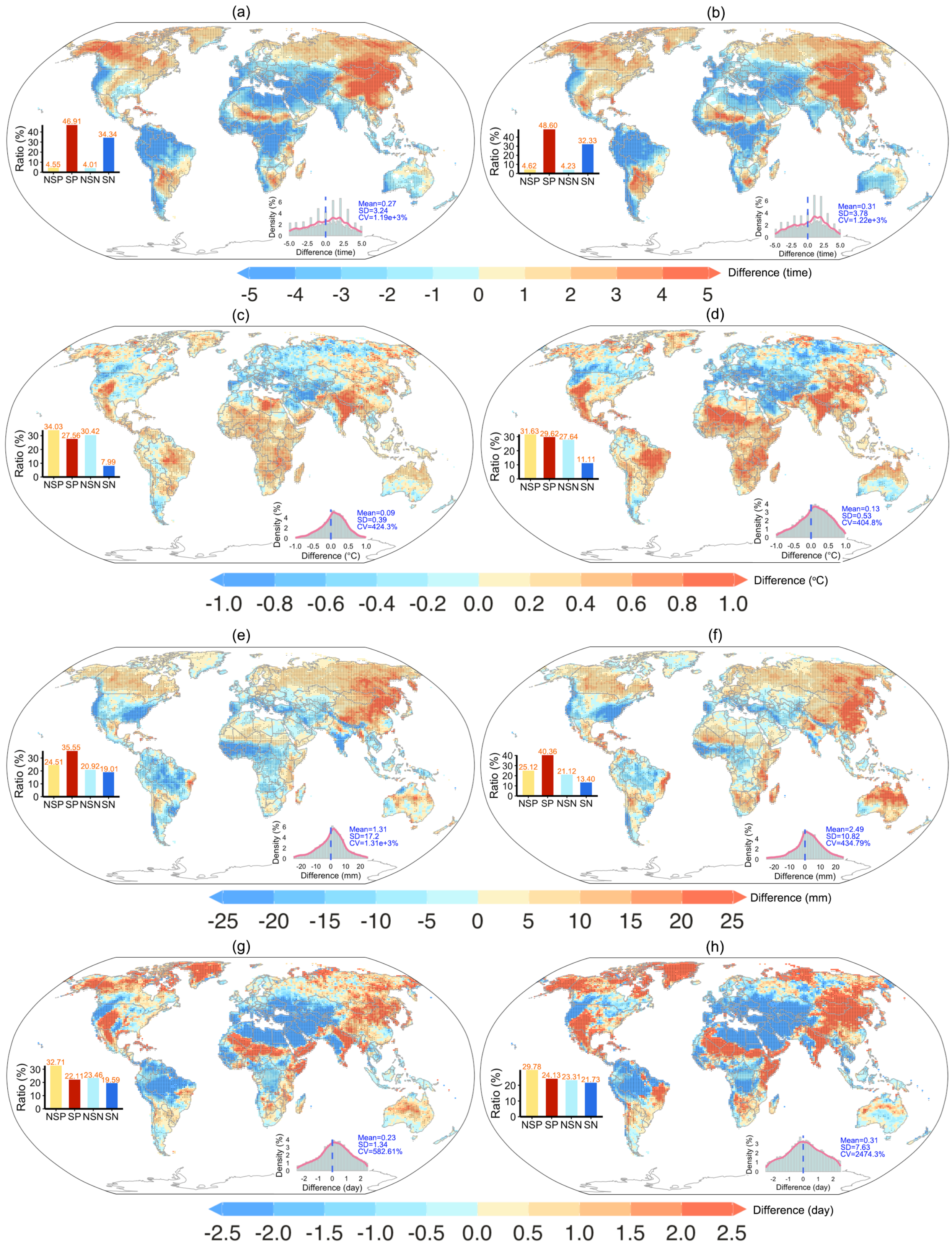

(a)
(b)
Difference (time)
-5 -4 -3 -2 -1 0 1 2 3 4 5
(c)
(d)
Difference (°C)
-1.0 -0.8 -0.6 -0.4 -0.2 0.0 0.2 0.4 0.6 0.8 1.0
(e)
(f)
Difference (mm)
-25 -20 -15 -10 -5 0 5 10 15 20 25
(g)
(h)
Difference (day)
-2.5 -2.0 -1.5 -1.0 -0.5 0.0 0.5 1.0 1.5 2.0 2.5

Figure 4. Spatial distribution of median differences between CHWEP and single extreme events in frequency (a and b), heatwave intensity (c and d), extreme precipitation intensity (e and f), and heatwave duration (g and h) from 2056 to 2100 under SSP2-4.5 (a, c, e, and g) and SSP5-8.5 (b, d, f, and h) scenarios.

Globally averaged trends in CHWEPs and single extreme events show that the frequency (Fig. 5a), heatwave intensity (Fig. 5b), extreme precipitation intensity (Fig. 5c), and heatwave duration (Fig. 5d) of both compound and single events are increasing over time. Notably, the rates of increase in frequency and heatwave duration are faster than those of heatwave intensity and extreme precipitation intensity. Furthermore, under the SSP5-8.5 scenario, all extreme event metrics are substantially higher than under the SSP2-4.5 scenario, indicating a strong dependence on the level of future warming.

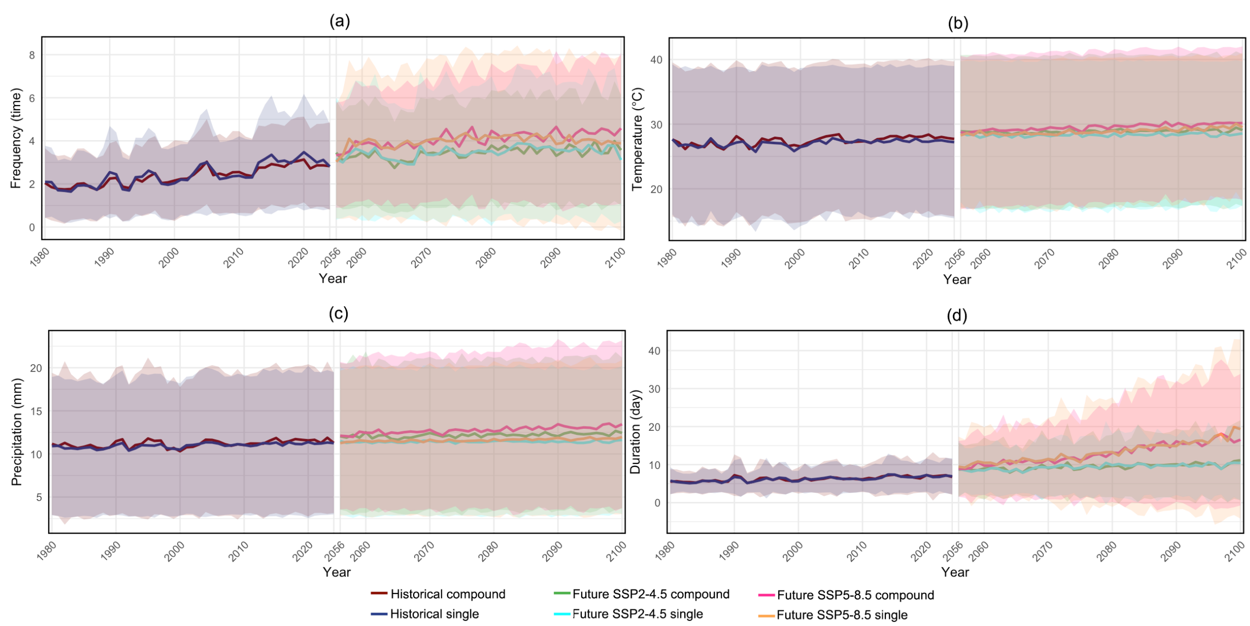

Figure 5. Changes in the frequency (a), heatwave intensity (b), extreme precipitation intensity (c), and heatwave duration (d) during the historical and future periods of CHWEP and single extreme events.

Compared to the historical period, both CHWEPs and single extreme events show increases in frequency, heatwave intensity, extreme precipitation intensity, and heatwave duration over more than half of the global land area under the SSP2-4.5 (Fig. S8) and SSP5-8.5 (Fig. S9) scenarios. The magnitude of these increases is substantially larger under the SSP5-8.5 scenario, indicating a strong dependence on the level of global warming. Box plots of the differences in metrics between the future and historical periods for CHWEP and single extreme events across different regions are shown in Fig. S10. The vast majority of metrics show some degree of increase across all continents.

Under the SSP2-4.5 and SSP5-8.5 scenarios, the proportion of grid cells showing positive changes in attribute metrics of CHWEP and single extreme events is overwhelmingly dominant. Under SSP5-8.5, the frequency (Fig. 6a), heatwave intensity (Fig. 6b), and heatwave duration (Fig. 6d) of both CHWEP and single extreme events are higher than under SSP2-4.5, with similar magnitudes of change. Furthermore, we find that under both scenarios, the extreme precipitation intensity associated with CHWEP is significantly greater than that of single extreme precipitation events (Fig. 6c). Notably, under SSP2-4.5, the precipitation intensity in CHWEP even exceeds that of single extreme events under the more severe SSP5-8.5 scenario. This indicates that CHWEP events feature stronger extreme precipitation, and heatwaves tend to amplify the intensity of concurrent rainfall extremes. This may be because rising temperatures accelerate the hydrological cycle, thereby promoting the occurrence of extreme precipitation, particularly in the mid- to high-latitude regions of the Northern Hemisphere.

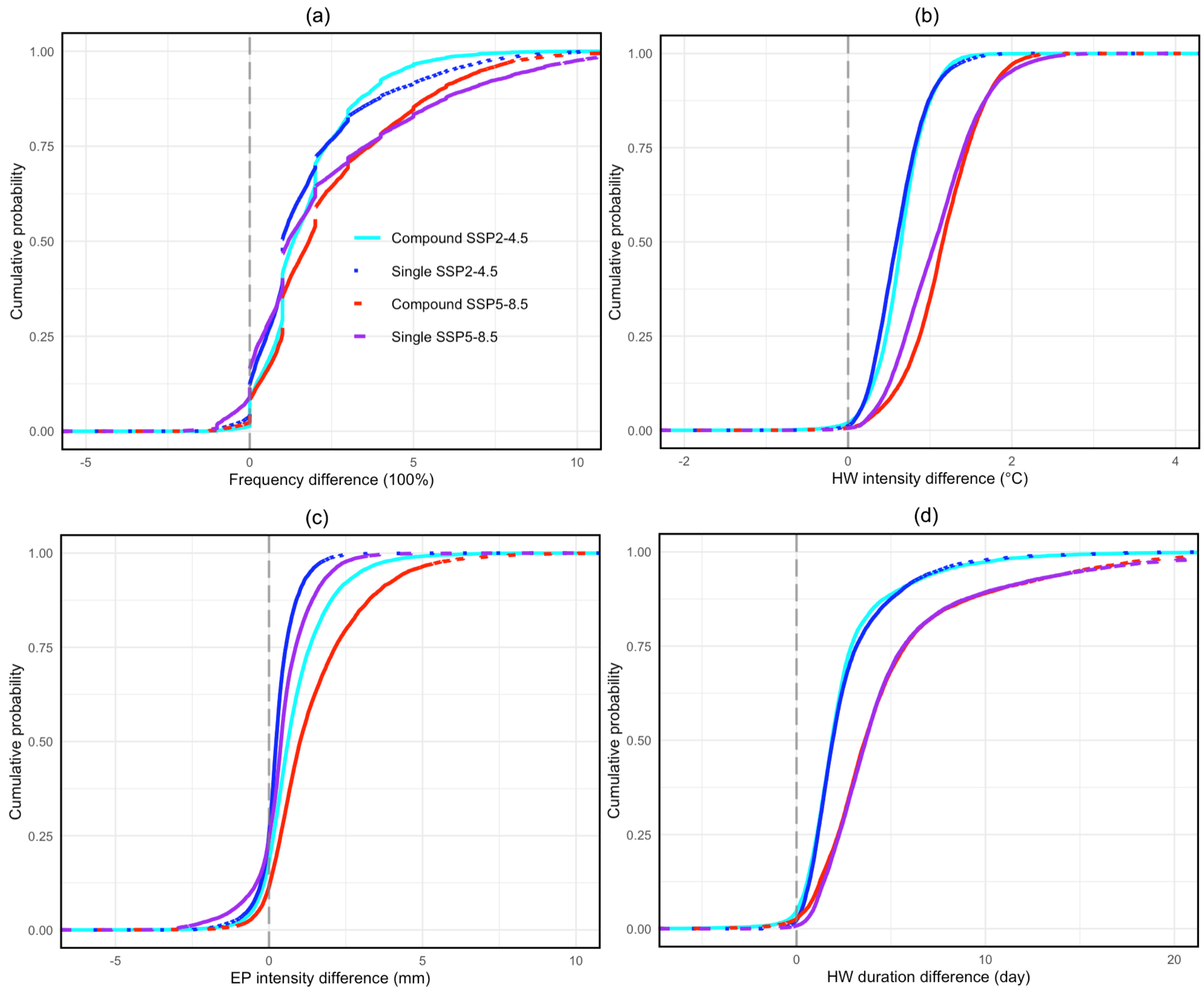

Figure 6. Comparison of the cumulative probability of the median differences between the frequency (a), heatwave intensity (b), extreme precipitation intensity (c), and heatwave duration (d) of CHWEP and single extreme events under the SSP2-4.5 and SSP5-8.5 scenarios and the historical period.

4.3 Probability of encountering heatwaves and extreme precipitation events

The observed probability of co-occurring heatwaves and extreme precipitation is higher in mid-to-high latitude regions (Fig. 7a), with smaller SDs, indicating lower variability (Fig. 7d). In contrast, the random probability of their co-occurrence is higher in tropical regions (Fig. 7b), but with greater variability (Fig. 7e). The ratio of observed to random probability exceeds 1 over more than 66% of the globe (Fig. 7c), particularly in mid-to-high latitudes, where the variability is relatively low (Fig. 7f), suggesting that heatwave events in these regions are more likely to be followed by extreme precipitation. In terms of trends, the observed probability (Fig. 7g), random probability (Fig. 7h), and their ratio (Fig. 7i) are increasing more rapidly in tropical regions, indicating a growing likelihood of CHWEP in the tropics in the future. Box plots of the observed probability and random probability along with their ratio, the SDs of both and the SD of their ratio, and the trends of both along with the trend of their ratio across different regions are shown in Fig. S11.

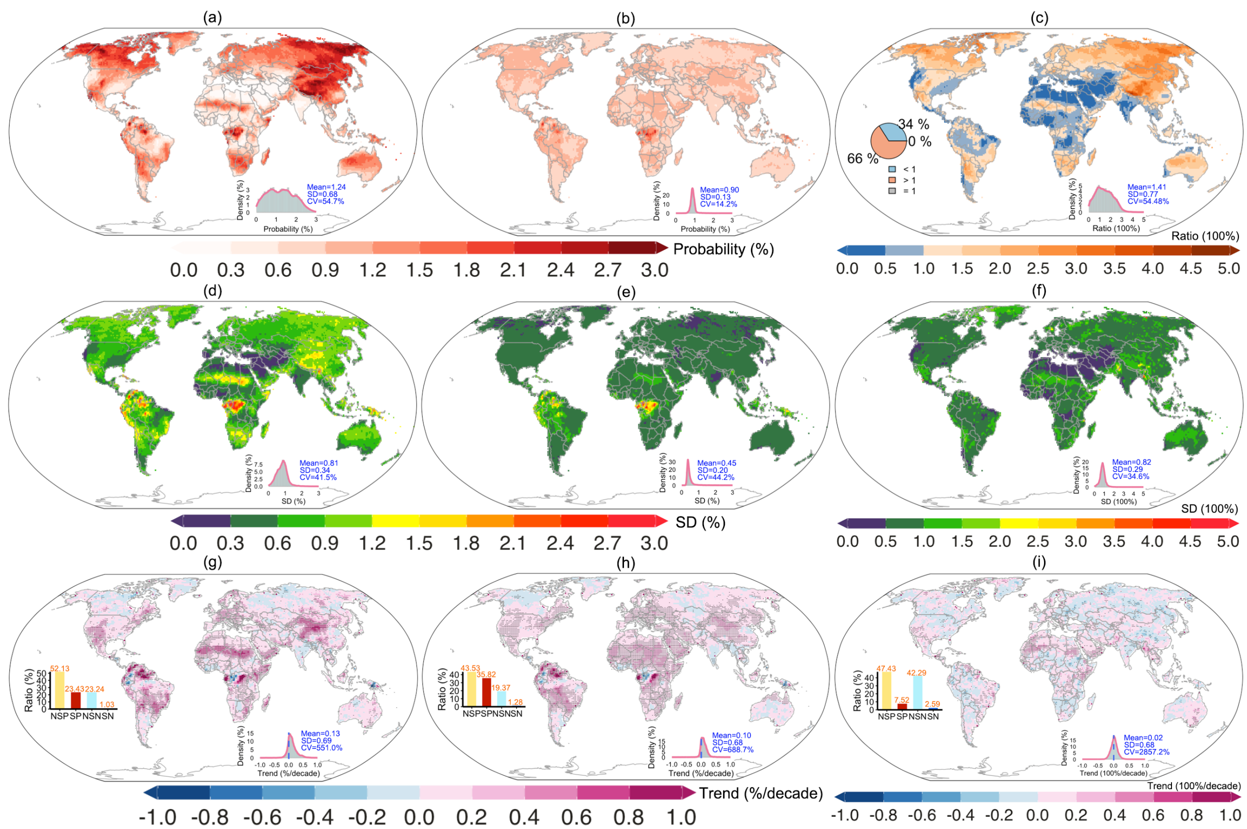

Figure 7. Spatial distributions of the mean observed probability (a), mean random probability (b), and mean ratio of observed probability to random probability over the period 1980-2024 in the first row (c), the second row shows the spatial distributions of their SDs (d-f), the third row presents their spatial patterns of linear trends (g-i).

In the future period, the observed probability of co-occurring heatwaves and extreme precipitation remains higher in mid-to-high latitude regions (Fig. 8a and d), while their random co-occurrence probability continues to be higher in tropical regions (Fig. 8b and e). Under the SSP5-8.5 scenario, both observed and random co-occurrence probabilities are notably higher than under the SSP2-4.5 scenario. Under SSP2-4.5, 70.9% of the globe shows a ratio of observed to random co-occurrence probability greater than 1 (Fig. 8c), increasing to 76.2% under SSP5-8.5 (Fig. 8f), indicating an intrinsic linkage mechanism between heatwaves and extreme precipitation. This suggests that, in the future, a growing number of regions worldwide will experience extreme precipitation following heatwave events. Box plots of the observed probability, random probability, and their ratio across different regions under the SSP2-4.5 and SSP5-8.5 scenarios are shown in Fig. S12.

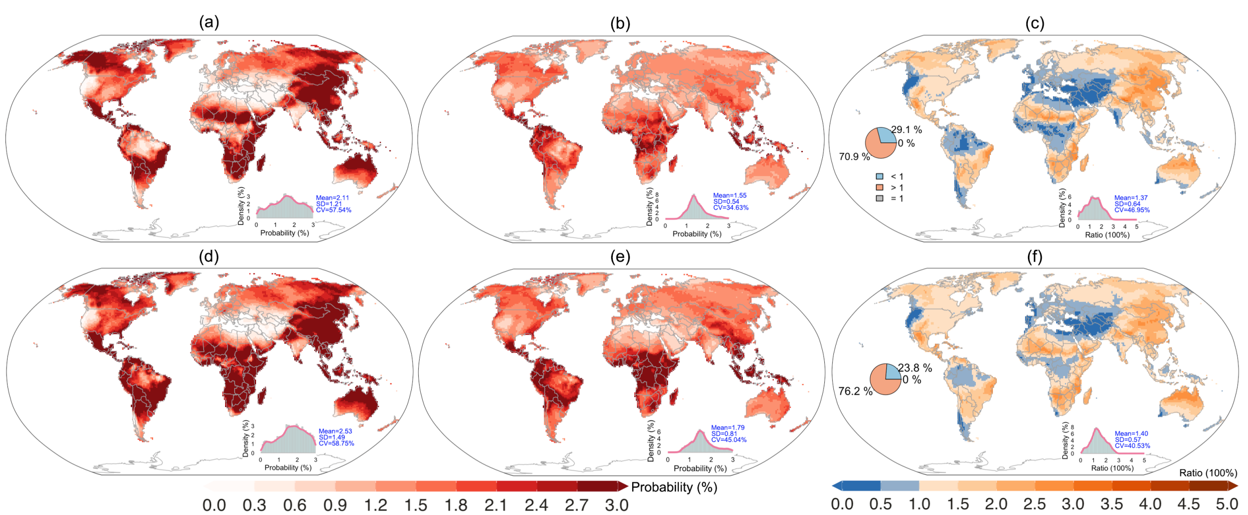

Figure 8. Spatial distributions of the mean observed probability (a and d), mean random probability (b and e), and mean ratio of observed probability to random probability (c and f) under the SSP2-4.5 (a-c) and SSP5-8.5 (d-f) scenarios for the period 2056-2100.

Globally, both the observed and random probabilities of heatwave and extreme precipitation co-occurrence show increasing trends from the historical period to the future period (Fig. 9a), with higher values and faster growth under the SSP5-8.5 scenario. This indicates that more CHWEP will occur globally under future climate change. Although both observed and random co-occurrence probabilities are rising, their ratio shows no significant trend over time, however, the ratio remains consistently greater than 1 (Fig. 9b). This demonstrates that CHWEP events are not merely the result of random coincidence, heatwaves tend to promote the subsequent occurrence of extreme precipitation, suggesting a physical linkage between the two extremes.

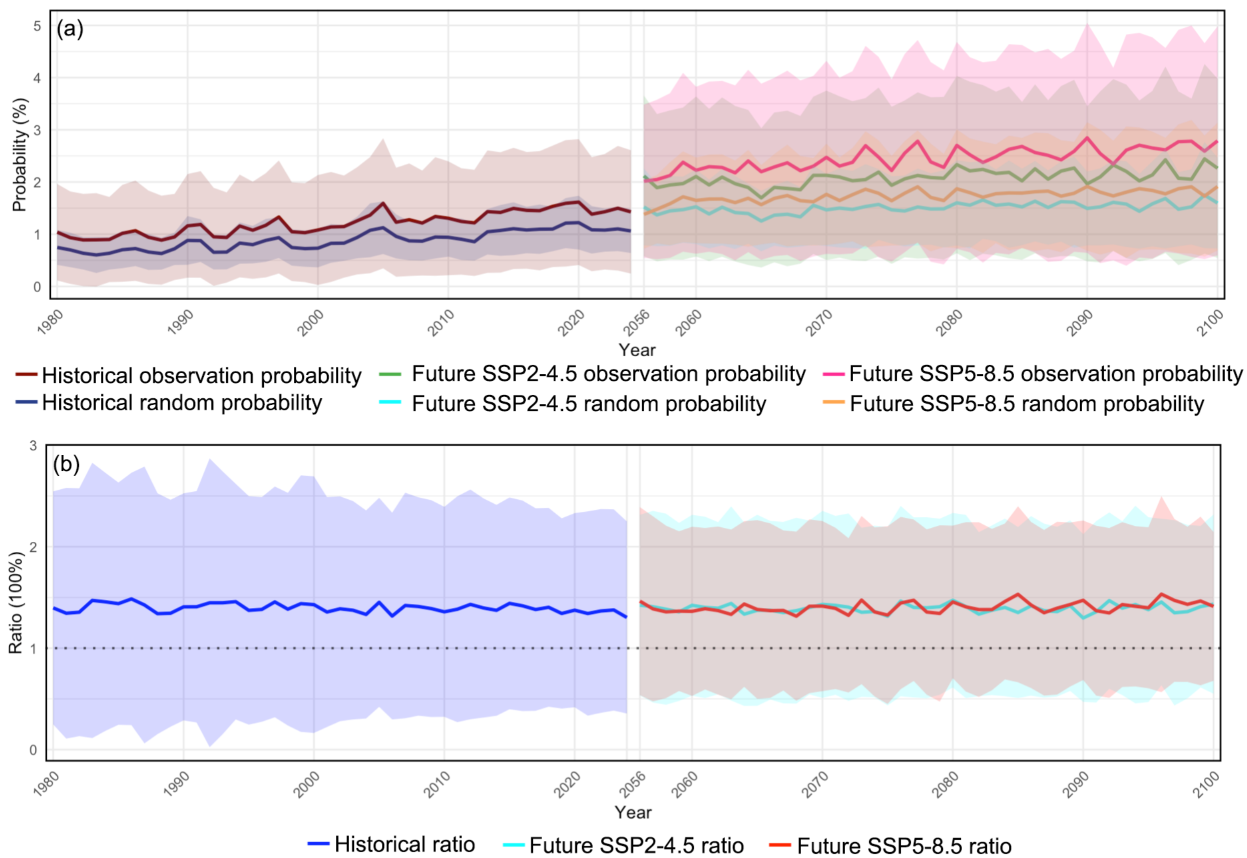

Figure 9. Changes in the observed probability and random probability (a), and their ratio (b) for the global co-occurrence of heatwaves and extreme precipitation between the historical period (1980-2024) and the future period (2056-2100).

Under future scenarios, the observed (Fig. 10a and d) and random (Fig. 10b and e) probabilities of heatwave and extreme precipitation co-occurrence increase over most of the globe, with larger increases in tropical regions. The magnitude of change in co-occurrence probability is greater under the SSP5-8.5 scenario than under SSP2-4.5. The ratio of observed to random co-occurrence probability (Fig. 10c and f) increases more in tropical regions but decreases in mid-to-high latitude regions, with larger changes under SSP5-8.5. This indicates that CHWEP events will become more frequent in the future, and the likelihood of extreme precipitation following heatwaves will increase more substantially in the tropics. Box plots of the differences in median values of observed probability, random probability, and their ratio for the co-occurrence of heatwaves and extreme precipitation between the future period (under SSP2-4.5 and SSP5-8.5 scenarios) and the historical period across different regions are shown in Fig. S13, with SAM and Africa exhibiting larger increases in both probability and ratio.

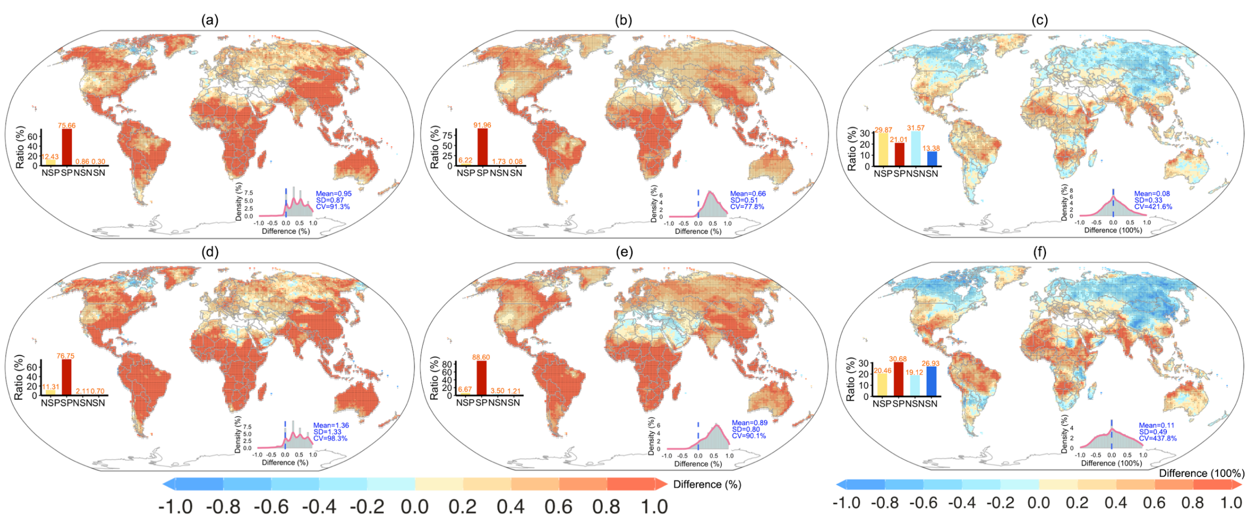

Figure 10. Spatial distribution of the differences in median values of observed probability (a and d), random probability (b and e), and their ratio (c and f) for the co-occurrence of heatwaves and extreme precipitation between the future period (under SSP2-4.5 (a-c) and SSP5-8.5 (d-f) scenarios) and the historical period.

5 Discussion

Compound extreme events are receiving increasing attention from both the scientific community and society, as regions experiencing concurrent or sequential extremes often face compounded or cascading impacts that lead to more severe socioeconomic and ecological damage than single extremes alone (Götte and Brunner, 2024; Sauter et al., 2023a; Sun et al., 2023). This study focuses on CHWEP, revealing that beyond the cumulative impact of sequential extremes, the integrated intensity of compound events exceeds that of individual extremes across most regions, resulting in heightened risks (Jin et al., 2024; Xiao et al., 2025). Previous studies suggest that the choice of extreme event thresholds and the time window for defining compound events have limited influence on the identification of their underlying linkages, whereas sufficient sample sizes enable more robust detection of long-term trends (Bevacqua et al., 2021; Diffenbaugh et al., 2017; Fang et al., 2025). Although climate models may exhibit biases in simulating absolute magnitudes, this study emphasizes relative changes, focusing on how compound events evolve rather than their exact intensity, ensuring the robustness of the findings (Chen et al., 2022; Ganguli and Merz, 2024; Lei et al., 2024).

This study shows that both CHWEP and single extreme events, such as single heatwaves or extreme precipitation, are increasing significantly in frequency, intensity, and duration. For example, both CHWEP and individual heatwave events show a greater increase in frequency in equatorial regions, CHWEP and individual heatwaves exhibit a larger increase in temperature intensity in the mid- to high-latitude regions of the Northern Hemisphere, CHWEP and individual extreme precipitation events display a more pronounced increase in precipitation intensity in equatorial regions, and the duration of CHWEP and individual heatwave events increases more substantially over the southwestern United States, the Sahara Desert, and India. These findings indicate that most regions of the globe are shifting toward a climate regime characterized by more frequent and more intense extreme weather events (Ning et al., 2022; Sun et al., 2024; Xiao et al., 2025). Crucially, the intensification of CHWEPs not only implies a higher risk of concurrent disasters but also reveals a dangerous "rapid transition" phenomenon, namely, a swift shift from extreme heat to extreme rainfall (Ning et al., 2022; Ridder et al., 2020; Tan et al., 2023; Xie and Zhou, 2023). These events reflect the dynamic linkage and rapid evolution between different types of extreme weather within the climate system, and have been increasingly observed in many regions worldwide in recent years, particularly prominent in the mid- to high-latitude areas (Donges et al., 2016; Tan et al., 2023; Zscheischler et al., 2020). The underlying physical mechanisms likely include: intense surface heating during heatwaves, which enhances atmospheric instability, and intensified evapotranspiration, which supplies additional moisture to the atmosphere (Bevacqua et al., 2021; Liao et al., 2021). When favorable large-scale circulation conditions, such as cold air intrusion or low-level jets occur, the accumulated energy and moisture are rapidly released, triggering strong convection and extreme precipitation (Cook et al., 2020; Jin et al., 2024; Lei et al., 2024). This abrupt transformation from drought-like heatwaves to flash flooding poses a severe challenge to traditional disaster preparedness systems, which are typically designed to address single-hazard events (Kumar et al., 2024; You and Wang, 2021; Zhou et al., 2023).

Furthermore, the spatiotemporal evolution patterns of compound and single extreme events revealed in this study provide critical scientific foundations for policymakers, urban planners, and emergency management agencies (Bevacqua et al., 2023; Gu et al., 2022; Myhre et al., 2019). By identifying high-risk regions and key temporal windows, relevant authorities can develop more resilient integrated early warning systems (Almeida et al., 2016; Dike et al., 2022; Sauter et al., 2023b). Advancing predictive models capable of capturing the transition from heatwaves to heavy rainfall is essential for effective water resource management, agricultural planning, public health response, and infrastructure safety (Kumar et al., 2024; Sun et al., 2023). In the context of climate change, where the synergistic and cascading nature of extreme events is intensifying, enhancing societal resilience and long-term sustainability in the face of compound climate disasters has become increasingly urgent and necessary (Miao et al., 2024; Sauter et al., 2023a; Woolway et al., 2021). In this study, we employed several methodological choices in our experimental design to enhance the robustness of our results, for instance, using the ensemble mean of multiple model outputs, defining extreme events based on the 90th percentile threshold, and applying a 7-day time window to identify event sequences, in order to obtain a sufficient number of extreme event samples. In future research, it would be beneficial to incorporate a larger number of climate models, test alternative percentile thresholds for defining extremes, and explore different time windows between consecutive extreme events to further validate the robustness and generalizability of our findings.

6 Conclusions

This study systematically analyzes the spatiotemporal evolution patterns of CHWEP and single extreme events. Results show that in mid-to-high latitude regions of the Northern Hemisphere, CHWEPs exhibit higher frequency, greater extreme precipitation intensity, and longer heatwave duration compared to single extremes. In tropical regions, the heatwave intensity within CHWEPs exceeds that of single heatwaves. These spatial contrasts persist under both future SSP2-4.5 and SSP5-8.5 scenarios. Compared to the historical period, metrics of both CHWEPs and single extremes increase across most of the globe in the future, with extreme precipitation following heatwaves becoming notably more intense than single extreme precipitation events.

Under the high-emission SSP5-8.5 scenario, the intensification of extremes is greater than under the moderate-emission SSP2-4.5 scenario. The co-occurrence of extreme precipitation after heatwaves is not merely a result of random coincidence. In the future, the likelihood of extreme precipitation following heatwaves will increase, particularly in tropical regions. These findings indicate that future CHWEP events will require increased attention, particularly with respect to ecosystem resilience and flood disaster prevention.

Code availability. All R codes can be provided by the corresponding authors upon request.

Data availability. The three global reanalysis datasets: ERA5 (https://cds.climate.copernicus.eu/datasets/derived-era5-land-daily-statistics?tab=download), MERRA-2 (https://disc.gsfc.nasa.gov/datasets/M2SDNXSLV_5.12.4/summary?keywords=merra2), and JRA-55 (https://jra.kishou.go.jp/JRA-55/index_en.html) can be accessed at the links. The four CMIP6 GCMs for the period 2056-2100, under two Shared Socioeconomic Pathway (SSP) scenarios: SSP2-4.5 and SSP5-8.5 can be accessed at https://aims2.llnl.gov/search/cmip6/.

Author contributions. KZ and HJ acquired the supervision and funding for this research. All authors contributed to the study conception, design, and methodology. ML, XY, and XY undertook the tasks of programming, data collection, result derivation, and interpretation. The original draft was prepared by HJ and ML and subsequently revised by LC, PZ and GL.

Competing interests. The contact author has declared that neither of the authors has any competing interests.

Acknowledgements. Data processing and visualization were performed with R (R Core Team, 2024). The authors express their gratitude to the reviewers.

Financial support. This study was supported by National Key Research and Development Program of China (2023YFC3006505), the Special Fund Project of Jiangsu Province Science and Technology Program (BZ2024035), the fund of National Key Laboratory of Water Disaster Prevention (524015222), the Project "Applied Scientific Research on the 'Three-Line Defense' Strengthening Foundation Project for Rainfall and Water Monitoring & Forecasting in Shandong Province" (370000000025001720240235), the Open Foundation of Beijige (BJG202513), and the Open Foundation of China Meteorological Administration Hydro-Meteorology Key Laboratory (Grant No. 24SWQXZ055).

References

Adeloye, A. J., Soundharajan, B.-S., Musto, J. N., and Chiamsathit, C.: Stochastic assessment of Phien generalized reservoir storage–yield–probability models using global runoff data records, J. Hydrol., 529, 1433–1441, https://doi.org/https://doi.org/10.1016/j.jhydrol.2015.08.038, 2015.

Almeida, A. T. de, Alencar, M. H., Garcez, T. V., and Ferreira, R. J. P.: A Systematic Literature Review of Multicriteria and Multi-Objective Models Applied in Risk Management, Ima J. Manag. Math., 28, 153–184, https://doi.org/10.1093/imaman/dpw021, 2016.

Babüroğlu, E. S., Durmuşoğlu, A., and Dereli, T.: Novel hybrid pair recommendations based on a large-scale comparative study of concept drift detection, Expert Syst. Appl., 163, 113786, https://doi.org/https://doi.org/10.1016/j.eswa.2020.113786, 2021.

Balaji, V., Taylor, K. E., Juckes, M., Lawrence, B., Durack, P. J., Lautenschlager, M., Blanton, C., Cinquini, L., Denvil, S., Elkington, M., Guglielmo, F., Guilyardi, É., Hassell, D., Kharin, S., Kindermann, S., Nikonov, S., Radhakrishnan, A., Stockhause, M., Weigel, T., and Williams, D. N.: Requirements for a Global Data Infrastructure in Support of CMIP6, Geosci. Model Dev., 11, 3659–3680, https://doi.org/10.5194/gmd-11-3659-2018, 2018.

Bevacqua, E., Michele, C. De, Manning, C., Couasnon, A., Ribeiro, A., Ramos, A. M., Vignotto, E., Bastos, A., Blesić, S., Durante, F., Hillier, J. K., Oliveira, S. C., Pinto, J. G., Ragno, E., Rivoire, P., Saunders, K., Wiel, K. van der, Wu, W., Zhang, T., and Zscheischler, J.: Guidelines for Studying Diverse Types of Compound Weather and Climate Events, Earth S Futur., 9, https://doi.org/10.1029/2021ef002340, 2021.

Bevacqua, E., Suarez-Gutierrez, L., Jézéquel, A., Lehner, F., Vrac, M., Yiou, P., and Zscheischler, J.: Advancing research on compound weather and climate events via large ensemble model simulations, Nat. Commun., 14, 2145, https://doi.org/10.1038/s41467-023-37847-5, 2023.

Chen, S., Gan, T. Y., Tan, X., Shao, D., and Zhu, J.: Assessment of CFSR, ERA-Interim, JRA-55, MERRA-2, NCEP-2 Reanalysis Data for Drought Analysis Over China, Clim. Dyn., 53, 737–757, https://doi.org/10.1007/s00382-018-04611-1, 2019.

Chen, Y., Liao, Z., Shi, Y., Li, P., and Zhai, P.: Greater Flash Flood Risks From Hourly Precipitation Extremes Preconditioned by Heatwaves in the Yangtze River Valley, Geophys. Res. Lett., 49, https://doi.org/10.1029/2022GL099485, 2022.

Dao, P.: On Wilcoxon rank sum test for condition monitoring and fault detection of wind turbines, Appl. Energy, https://doi.org/10.1016/j.apenergy.2022.119209, 2022.

Diffenbaugh, N., Singh, D., Mankin, J., Horton, D., Swain, D., Touma, D., Charland, A., Liu, Y., Haugen, M., Tsiang, M., and Rajaratnam, B.: Quantifying the influence of global warming on unprecedented extreme climate events, Proc. Natl. Acad. Sci., 114, 4881–4886, https://doi.org/10.1073/pnas.1618082114, 2017.

Dike, V. N., Lin, Z., Fei, K., Langendijk, G. S., and Nath, D.: Evaluation and Multimodel Projection of Seasonal Precipitation Extremes Over Central Asia Based on CMIP6 Simulations, Int. J. Climatol., 42, 7228–7251, https://doi.org/10.1002/joc.7641, 2022.

Donges, J. F., Schleussner, C.-F., Siegmund, J. F., and Donner, R. V: Event coincidence analysis for quantifying statistical interrelationships between event time series, Eur. Phys. J. Spec. Top., 225, 471–487, https://doi.org/10.1140/epjst/e2015-50233-y, 2016.

Fang, P., Wang, T., Yang, D., Tang, L., and Yang, Y.: Substantial increases in compound climate extremes and associated socio-economic exposure across China under future climate change, npj Clim. Atmos. Sci., 8, 17, https://doi.org/10.1038/s41612-025-00910-7, 2025.

Fischer, E. M. and Knutti, R.: Anthropogenic contribution to global occurrence of heavy-precipitation and high-temperature extremes, Nat. Clim. Chang., 5, 560–564, https://doi.org/10.1038/nclimate2617, 2015.

Ganguli, P. and Merz, B.: Observational Evidence Reveals Compound Humid Heat Stress-Extreme Rainfall Hotspots in India, Earth's Futur., 12, e2023EF004074, https://doi.org/https://doi.org/10.1029/2023EF004074, 2024.

Götte, J. and Brunner, M. I.: Hydrological Drought-To-Flood Transitions Across Different Hydroclimates in the United States, Water Resour. Res., 60, https://doi.org/10.1029/2023wr036504, 2024.

Gu, L., Chen, J., Yin, J., Slater, L., Wang, H., Guo, Q., Feng, M., Qin, H., and Zhao, T.: Global Increases in Compound Flood-Hot Extreme Hazards Under Climate Warming, Geophys. Res. Lett., 49, https://doi.org/10.1029/2022GL097726, 2022.

Guerreiro, S. B., Fowler, H. J., Barbero, R., Westra, S., Lenderink, G., Blenkinsop, S., Lewis, E., and Xiao-feng, L. I.: Detection of Continental-Scale Intensification of Hourly Rainfall Extremes, Nat. Clim. Chang., 8, 803–807, https://doi.org/10.1038/s41558-018-0245-3, 2018.

Hausfather, Z., Marvel, K., Schmidt, G.A., Nielsen-Gammon, J.W., Zelinka, M., 2022. Climate simulations: recognize the 'hot model' problem. Nature 605, 26–29. https://doi.org/10.1038/d41586-022-01192-2

Huang, D., Jian, Z., Zhang, Y., Huang, Y., and Kuang, X.: Assessment of Summer Monsoon Precipitation Derived From Five Reanalysis Datasets Over East Asia, Q. J. R. Meteorol. Soc., 142, 108–119, https://doi.org/10.1002/qj.2634, 2015.

Jin, K., Wu, Y., Sun, X., Sun, Y., and Gao, C.: Spatial-Temporal Assessment of Future Population Exposure to Compound Extreme Precipitation-High Temperature Events Across China, PLoS One, 19, e0307494, https://doi.org/10.1371/journal.pone.0307494, 2024.

Juckes, M., Taylor, K. E., Durack, P. J., Lawrence, B., Mizielinski, M., Pamment, A., Peterschmitt, J.-Y., Rixen, M., and Sénési, S.: The CMIP6 Data Request (DREQ, Version 01.00.31), Geosci. Model Dev., 13, 201–224, https://doi.org/10.5194/gmd-13-201-2020, 2020.

KOBAYASHI, S., OTA, Y., HARADA, Y., EBITA, A., MORIYA, M., ONODA, H., ONOGI, K., KAMAHORI, H., KOBAYASHI, C., ENDO, H., MIYAOKA, K., and TAKAHASHI, K.: The JRA-55 Reanalysis: General Specifications and Basic Characteristics, J. Meteorol. Soc. Japan. Ser. II, 93, 5–48, https://doi.org/10.2151/jmsj.2015-001, 2015.

Kumar, V., Kedam, N., Kişi, Ö., Alsulamy, S., Khedher, K. M., and Salem, M. A.: A Comparative Study of Machine Learning Models for Daily and Weekly Rainfall Forecasting, Water Resour. Manag., 39, 271–290, https://doi.org/10.1007/s11269-024-03969-8, 2024.

Lei, H., Ma, Q., Chang, Y., Gu, Y., Wan, S., Zhu, Z., and Feng, G.: Multiscale Interactions Driving Summer Extreme Precipitation in Central Asia, Geophys. Res. Lett., 51, https://doi.org/10.1029/2024gl108882, 2024.

Li, C., Wei, W., Chan, P., and Huang, J.: Heatwaves in Hong Kong and their influence on pollution and extreme precipitation, Atmos. Res., https://doi.org/10.1016/j.atmosres.2024.107845, 2025.

Liu, J., Chen, J., Yin, J., Su, T., Xiong, L., and Xia, J.: Understanding compound extreme precipitations preconditioned by heatwaves over China under climate change, Environ. Res. Lett., 19, https://doi.org/10.1088/1748-9326/ad50ee, 2024.

Mazdiyasni, O. and AghaKouchak, A.: Substantial Increase in Concurrent Droughts and Heatwaves in the United States, Proc. Natl. Acad. Sci., 112, 11484–11489, https://doi.org/10.1073/pnas.1422945112, 2015.

Miao, L., Ju, L., Sun, S., Agathokleous, E., Wang, Q., Zhu, Z., Liu, R., Zou, Y., Lu, Y., and Liu, Q.: Unveiling the dynamics of sequential extreme precipitation-heatwave compounds in China, npj Clim. Atmos. Sci., 7, 67, https://doi.org/10.1038/s41612-024-00613-5, 2024.

Myhre, G., Alterskjær, K., Stjern, C. W., Hodnebrog, Ø., Marelle, L., Samset, B. H., Sillmann, J., Schaller, N., Fischer, E., Schulz, M., and Stohl, A.: Frequency of extreme precipitation increases extensively with event rareness under global warming, Sci. Rep., 9, 16063, https://doi.org/10.1038/s41598-019-52277-4, 2019.

Ning, G., Luo, M., Zhang, W., Liu, Z., Wang, S., and Gao, T.: Rising Risks of Compound Extreme Heat-precipitation Events in China, Int. J. Climatol., 42, 5785–5795, https://doi.org/10.1002/joc.7561, 2022.

Raghavendra, A., Dai, A., Milrad, S., and Cloutier-Bisbee, S.: Floridian heatwaves and extreme precipitation: future climate projections, Clim. Dyn., 52, 495–508, https://doi.org/10.1007/s00382-018-4148-9, 2018.

Ridder, N. N., Pitman, A. J., Westra, S., Ukkola, A., Do, H. X., Bador, M., Hirsch, A. L., Evans, J. P., Di Luca, A., and Zscheischler, J.: Global hotspots for the occurrence of compound events, Nat. Commun., 11, 5956, https://doi.org/10.1038/s41467-020-19639-3, 2020.

Sauter, C., Fowler, H. J., Westra, S., Ali, H., Peleg, N., and White, C. J.: Compound extreme hourly rainfall preconditioned by heatwaves most likely in the mid-latitudes, Weather Clim. Extrem., 40, 100563, https://doi.org/https://doi.org/10.1016/j.wace.2023.100563, 2023a.

Sauter, C., Catto, J. L., Fowler, H. J., Westra, S., and White, C. J.: Compounding Heatwave-Extreme Rainfall Events Driven by Fronts, High Moisture, and Atmospheric Instability, J. Geophys. Res. Atmos., 128, e2023JD038761, https://doi.org/https://doi.org/10.1029/2023JD038761, 2023b.

Séférian, R., Nabat, P., Michou, M., Saint-Martin, D., Voldoire, A., Colin, J., Decharme, B., Delire, C., Berthet, S., Chevallier, M., Sénési, S., Franchistéguy, L., Vial, J., Mallet, M., Joetzjer, É., Geoffroy, O., Guérémy, J., Moine, M., Msadek, R., Ribes, A., Rocher, M., Roehrig, R., Salas-y-Mélia, D., Sanchez, E., Terray, L., Valcke, S., Waldman, R., Aumont, O., Bopp, L., Deshayes, J., Éthé, C., and Madec, G.: Evaluation of CNRM Earth System Model, CNRM-ESM2-1: Role of Earth System Processes in Present-Day and Future Climate, J. Adv. Model. Earth Syst., 11, 4182–4227, https://doi.org/10.1029/2019ms001791, 2019.

Sun, P., Zou, Y., Yao, R., Bian, Y., Ge, C., and Lv, Y.: Compound and successive events of extreme precipitation and extreme runoff under heatwaves based on CMIP6 models., Sci. Total Environ., 162980, https://doi.org/10.1016/j.scitotenv.2023.162980, 2023.

Sun, P., Bian, Y., Yu, S., Yao, R., Wang, Z., Zhang, Q., Chen, W., Ge, C., Ma, Z., and Du, W.: Are longer and more intense heatwaves more prone to extreme precipitation?, Glob. Planet. Change, 236, 104428, https://doi.org/https://doi.org/10.1016/j.gloplacha.2024.104428, 2024.

Tan, X., Wu, X., Huang, Z., Fu, J., Tan, X., Deng, S., Liu, Y., Gan, T. Y., and Liu, B.: Increasing global precipitation whiplash due to anthropogenic greenhouse gas emissions, Nat. Commun., 14, 2796, https://doi.org/10.1038/s41467-023-38510-9, 2023.

Wang, G., Zhang, X., and Zhang, S.: Performance of Three Reanalysis Precipitation Datasets Over the Qinling-Daba Mountains, Eastern Fringe of Tibetan Plateau, China, Adv. Meteorol., 2019, 1–16, https://doi.org/10.1155/2019/7698171, 2019a.

Wang, S., Kim, H., Coumou, D., Yoon, J., Zhao, L., and Gillies, R. R.: Consecutive Extreme Flooding and Heat Wave in Japan: Are They Becoming a Norm?, Atmos. Sci. Lett., 20, https://doi.org/10.1002/asl.933, 2019b.

Woolway, R. I., Kraemer, B. M., Zscheischler, J., and Albergel, C.: Compound Hot Temperature and High Chlorophyll Extreme Events in Global Lakes, Environ. Res. Lett., 16, 124066, https://doi.org/10.1088/1748-9326/ac3d5a, 2021.

Xiao, R., Liu, R., Xie, X., Xu, Y., Bi, Y., and Zhang, W.: Characteristics and evolution of heat wave and extreme precipitation compound events in South China based on copula function, Q. J. R. Meteorol. Soc., n/a, e5055, https://doi.org/https://doi.org/10.1002/qj.5055, 2025.

Xie, W. and Zhou, B.: On the Atmospheric Background for the Occurrence of Three Heat Wave Types in East China, Weather Clim. Extrem., 39, 100539, https://doi.org/10.1016/j.wace.2022.100539, 2023.

Xiong, J., Guo, S., Wu, Y., Yan, D., Xiao, C., and Lu, X.: Predicting the Response of Heating and Cooling Demands of Residential Buildings With Various Thermal Performances in China to Climate Change, Energy, 269, 126789, https://doi.org/10.1016/j.energy.2023.126789, 2023.

Yang, Y. and Yuan, C.: Causality of compound extreme heat-precipitation events in Northeastern China, Atmos. Res., https://doi.org/10.1016/j.atmosres.2025.107975, 2025.

You, J. and Wang, S.: Higher Probability of Occurrence of Hotter and Shorter Heat Waves Followed by Heavy Rainfall, Geophys. Res. Lett., 48, https://doi.org/10.1029/2021gl094831, 2021.

Zhao, H., Zhang, L., Kirkham, M. B., Welch, S. M., Nielsen-Gammon, J. W., Bai, G., Luo, J., Andresen, D., Rice, C. W., Wan, N., Lollato, R. P., Zheng, D., Gowda, P. H., and Lin, X.: U.S. Winter Wheat Yield Loss Attributed to Compound Hot-Dry-Windy Events, Nat. Commun., 13, https://doi.org/10.1038/s41467-022-34947-6, 2022.

Zhou, W., Liu, D., Zhang, J., Jiang, S., Shu-ying, X., Wang, J., Cheng, Y., and Chen, N.: Identification and Frequency Analysis of Drought–flood Abrupt Alternation Events Using a Daily-Scale Standardized Weighted Average of the Precipitation Index, Front. Environ. Sci., 11, https://doi.org/10.3389/fenvs.2023.1142259, 2023.

Zscheischler, J., Westra, S., Hurk, B. van den, Seneviratne, S. I., Ward, P. J., Pitman, A. J., AghaKouchak, A., Bresch, D. N., Leonard, M., Wahl, T., and Zhang, X.: Future Climate Risk From Compound Events, Nat. Clim. Chang., 8, 469–477, https://doi.org/10.1038/s41558-018-0156-3, 2018.

Zscheischler, J., Martius, O., Westra, S., Bevacqua, E., Raymond, C., Horton, R., Hurk, B. van den, AghaKouchak, A., Jézéquel, A., Mahecha, M. D., Maraun, D., Ramos, A. M., Ridder, N., Thiery, W., and Vignotto, E.: A Typology of Compound Weather and Climate Events, Nat. Rev. Earth Environ., 1, 333–347, https://doi.org/10.1038/s43017-020-0060-z, 2020.